uicc
global cancer control

IJC
International Journal of Cancer

Identification of a novel recurrent 1q42.2-1qter deletion in high risk *MYCN* single copy 11q deleted neuroblastomas

Annelies Fieuw[1], Candy Kumps[1], Alexander Schramm[2], Filip Pattyn[1], Björn Menten[1], Francesca Antonacci[3], Peter Sudmant[3], Johannes H. Schulte[2], Nadine Van Roy[1], Sarah Vergult[1], Patrick G. Buckley[4,5], Anne De Paepe[1], Rosa Noguera[6], Rogier Versteeg[7], Raymond Stallings[4], Angelika Eggert[2], Jo Vandesompele[1], Katleen De Preter[1] and Frank Speleman[1]

[1] Center for Medical Genetics, Ghent University Hospital, Ghent, Belgium
[2] Department of Pediatric Oncology and Haematology, University Children's Hospital Essen, Essen, Germany
[3] Eichler Lab, Department of Genome Sciences, University of Washington, Seattle, WA
[4] Department of Cancer Genetics, Royal College of Surgeons in Ireland and National Children's Research Centre, Our Lady's Children's Hospital, Dublin, Ireland
[5] Department of Molecular and Cellular Therapeutics, The Royal College of Surgeons in Ireland, Ireland
[6] Department of Pathology, Medical School, University of Valencia, Valencia, Spain
[7] Department of Human Genetics, Academic Medical Center, University of Amsterdam, Amsterdam, The Netherlands

Neuroblastoma is an aggressive embryonal tumor that accounts for ~15% of childhood cancer deaths. Hitherto, despite the availability of comprehensive genomic data on DNA copy number changes in neuroblastoma, relatively little is known about the genes driving neuroblastoma tumorigenesis. In this study, high resolution array comparative genome hybridization (CGH) was performed on 188 primary neuroblastoma tumors and 33 neuroblastoma cell lines to search for previously undetected recurrent DNA copy number gains and losses. A new recurrent distal chromosome 1q deletion (del(1)(q42.2qter)) was detected in seven cases. Further analysis of available array CGH datasets revealed 13 additional similar distal 1q deletions. The majority of all detected 1q deletions was found in high risk 11q deleted tumors without *MYCN* amplification (Fisher exact test $p = 5.61 \times 10^{-5}$). Using ultra-high resolution (~115 bp resolution) custom arrays covering the breakpoints on 1q for 11 samples, clustering of nine breakpoints was observed within a 12.5-kb region, of which eight were found in a 7-kb copy number variable region, whereas the remaining two breakpoints were colocated 1.4-Mb proximal. The commonly deleted region contains one miRNA (hsa-mir-1537), four transcribed ultra conserved region elements (uc.43-uc.46) and 130 protein coding genes including at least two *bona fide* tumor suppressor genes, *EGLN1* (or *PHD2*) and *FH*. This finding further contributes to the delineation of the genomic profile of aggressive neuroblastoma, offers perspectives for the identification of genes contributing to the disease phenotype and may be relevant in the light of assessment of response to new molecular treatments.

Neuroblastoma (NB) is the most common extracranial solid tumor in children and arises from sympathetic neural crest progenitor cells.[1,2] In contrast to pediatric leukemias for which survival rates have dramatically increased over the past decades, the overall survival in high risk NB subgroups is still disappointingly low.[1] Understanding the molecular pathology of NB can open the way to more efficient and less toxic targeted therapies. Recent advances in the genomic characterization of various malignancies including NB have already shown that the identification of causal genes and perturbed pathways in

Key words: neuroblastoma, array CGH, chromosome 1, deletion

Abbreviations: array CGH: array comparative genome hybridization; EGLN1: egl nine homolog 1; FISH: fluorescence *in situ* hybridization; FH: fumarate hydratase; miRNA: microRNA; NB: neuroblastoma; NBGS: neuroblastoma gene server; PHD2: prolyl hydroxylase domain protein 2; SDHB: succinate dehydrogenase, subunit B; SDHD: succinate dehydrogenase, subunit D; T-UCR: transcribed ultra conserved region; VHL: von-Hippel Lindau; WGAC: whole genome assembly comparison; WSSC: whole genome shotgun sequence detection
Additional Supporting Information may be found in the online version of this article.

Grant sponsor: Institute for the Promotion of Innovation by Science and Technology in Flandres (IWT); **Grant number:** SB060848; **Grant sponsor:** Fund for Scientific Research (FWO); **Grant number:** G.0198.08; **Grant sponsor:** GOA; **Grant number:** 01G01910; **Grant sponsor:** ISCII and ERDF (Spain); **Grant number:** RD06/0020/0202; **Grant sponsor:** Science Foundation Ireland; **Grant number:** 07/IN.1/B1776
DOI: 10.1002/ijc.26317
History: Received 12 Apr 2011; Accepted 12 Jul 2011; Online 27 jul 2011

Correspondence to: Frank Speleman, Center for Medical Genetics, Ghent University Hospital, De Pintelaan 185, B-9000 Ghent, Belgium, Tel.:+32 9 332 2451, Fax: +32-9-332-6549, E-mail: franki.speleman@ugent.be

tumors can pave the way toward innovative therapies such as Gleevec,[3] Erlotinib[4] and Nutlin.[5] As was recently illustrated by the case of increased proliferative effect of BRAF-selective inhibitors in RAS mutant melanomas,[6] in depth knowledge of pathway signaling in relation to the comprehensive genomic profile of individual tumors may be required prior to administrating drugs for targeted therapy. Detailed molecular portraits through high density genomic DNA arrays and genome wide mutation profiles will aid in understanding the molecular basis of individual responses to new molecular therapies. While whole genome sequencing efforts for NB are underway, DNA copy number analyses have already provided an extensive insight into the genetic heterogeneity of NB. Overall, based on genomic profiles, the majority of NB samples can be grouped into three major subtypes linked to prognosis[7–10]: Subtype 1 consisting of mainly numerical aberrations with favorable prognosis; Subtype 2A with 17q gain and 11q loss, often in combination with a 3p loss but without *MYCN* amplification and Subtype 2B with *MYCN* amplification, 1p deletion and 17q gain. The latter two subtypes are associated with an unfavorable prognosis. Furthermore, higher resolution array CGH analyses have also uncovered the presence of additional focal recurrent DNA copy number alterations affecting genes implicated in the *MYCN* pathway, apoptosis and differentiation (Kumps *et al.*, unpublished data).

As a result of our search for new recurrent DNA copy number alterations in NB, we discovered a previously unnoticed recurrent distal chromosome 1q deletion. This deletion occurs predominantly in high risk *MYCN* single copy NB with 11q deletions. Interestingly, breakpoint analysis using ultra-high resolution array CGH showed that in eight out of 11 cases breakpoints clustered to a 7-kb copy number variable region indicating that the underlying genomic architecture may have triggered the formation of this recurrent intrachromosomal 1q rearrangement. The deleted region encompasses multiple gene loci including several tumor suppressor genes.

Material and Methods

Primary NB tumors and cell lines

A cohort of 188 primary NB tumors (54 samples from Ghent University Hospital, Belgium; 33 samples from the Medical School of Valencia, Spain; 101 samples from Essen University Children's Hospital, Germany) and an additional panel of 33 NB cell lines were included in this study. Clinical and genomic information regarding these samples is summarized in Supporting Information Table 1.

DNA isolation

DNA was isolated from all primary tumors and cell lines using the QIAamp DNA mini kit (Qiagen), as specified in the manufacturer's protocol.

Array CGH analysis

All samples were profiled on a 44 or 60 K custom designed oligonucleotide array platform (157 samples and 64 samples, respectively). These arrays were selectively enriched for genomic regions known to be recurrently implicated in NB, such as 1p, 2p, 3p, 11q and 17. Furthermore, oligonucleotides encompassing miRNA loci and transcribed ultraconserved region elements (T-UCRs), as well as cancer gene census genes and genes from the Neuroblastoma Gene Server Database (http://medgen.ugent.be/NBGS/; Pattyn *et al.*, unpublished data) were added to the custom array.

A specific ultra-high density array was designed, containing 47,091 probes within a 5.4 Mb segment surrounding the distal 1q deletion breakpoint, creating a resolution of ~115 bp. Eleven tumors with a distal 1q deletion were profiled on this platform, to further delineate the breakpoint regions.

An ultrahigh resolution 1M array platform (~3-kb resolution) was used for the profiling of the NB cell line SK-N-FI.

The array CGH analysis was performed by hybridizing 400, 200, or 1,000 ng (for 44K, 60K or 1M array, respectively) of tumor DNA against an equal amount of control human reference DNA (male promega control DNA, male EBV99 cell line DNA or female EBV411 cell line DNA, see Supporting Information Table 1), after random primer labeling with Cy3 and Cy5 dyes (Perkin Elmer). The proceeding steps in the hybridization protocol were done according to the manufacturer's instructions (Agilent Technologies). After scanning (G2505C Agilent scanner, Agilent Technologies) and extraction of the features (feature extraction v10.1.1.1 software), further processing of the data included the circular binary segmentation algorithm (CBS),[11] for the delineation of the chromosomal gains and losses, and the wave correction algorithm,[12] both of which are implemented in the in-house developed array CGH software arrayCGHbase (http://medgen.ugent.be/arraycghbase).[13] For the array profiles generated on the 1M and custom 1q platform the wave correction algorithm was not implemented.

All array CGH data are made available at http://medgen.ugent.be/arraycghbase/ (login guest, password guest). All base pair positions are referring to human genome build 36 (hg18).

Data mining and statistical analysis

After extraction of wave corrected CBS ratio values from arrayCGHbase, the statistical software R (2.10.0) was used to automate the identification of recurrent and/or frequent aberrations and to perform statistical analysis on the obtained data. Fisher exact test was used to determine the association of the 1q deletion with clinical and genomic parameters. Kaplan–Meier curves were plotted for the visualization of survival data for the different NB subtypes. Survival data from 177 of the patients from our cohort (of which 6 with 1q deletion) were available for these survival analyses. A cut-off $\log_2$ value of -0.3 or 0.3 was implemented for the identification of losses or gains, respectively.

Fluorescence in situ hybridization (FISH)

Fluorescence *in situ* hybridization was performed on the SK-N-FI cell line, to confirm the distal 1q deletion. Two probes

proximal to the deletion breakpoint (RP11-379G13, RP11-118A16), and two probes distal to the breakpoint (RP11-27F05, RP11-641H04) were cohybridized with a Chromosome 1 specific probe (CEP 1; Abbott Laboratories, IL). FISH analysis was performed as described previously.[14]

Multiplex FISH (M-FISH) was performed on the SK-N-FI cell line as described previously.[15]

DNA sequencing

For two candidate tumor suppressor genes residing in the 1q deletion region, *FH* (fumarate hydratase) and *EGLN1* (EGL nine homolog 1, also referred to as *PHD2,* prolyl hydroxylase domain 2), mutation analysis of the coding exons was performed on genomic DNA of 32 NB cell lines and 9 primary tumors. Part of the first exon of *EGLN1* could not be amplified due to the presence of a GC rich region. Unidirectional Sanger sequencing was performed using an ABI3730XL sequencer (Applied Biosystems). Analysis of the results was performed with the Sequence Scanner v1.0 software (Applied Biosystems). The sequence of the primers that were used for this sequencing analysis can be found in Supporting Information Table 2.

mRNA expression analysis

A previously published gene expression dataset (GSE21713),[16] including a part of the samples profiled in this study, was used for the Spearman correlation analysis between copy number and expression of the genes in the 1q deleted region. In addition, specific expression analysis of the *H2AFX* gene for the different NB subgroups was performed on this dataset.

This dataset consists of 101 NB tumor samples of which five have distal 1q deletion.

miRNA expression analysis

Expression profiling was performed for hsa-mir-1182, a microRNA in close proximity of the breakpoint, and hsa-mir-1537, a miRNA residing in the distal 1q deletion region, using TaqMan microRNA assays as described earlier.[17,18] A total of 34 NB tumor samples with different stages were selected including four 1q deleted primary tumors as well as the SK-N-FI cell line with 1q deletion (Supporting Information Table 3).

In silico breakpoint analysis

In silico sequence analysis was performed to find sequence similarities between the distal 1q region encompassing the two breakpoint clusters and the surrounding region. The telomeric subsequence of Chromosome 1 from base position 225 904 200 (2-Mb upstream of the proximal breakpoint cluster) to 231 333 895 (2-Mb downstream of the distal breakpoint cluster) was retrieved from the human genome build 36 (hg18). The sequence was aligned part by part (every 10 bp) to the entire part of the genome under study, in this case the 5.4-Mb region, whereby exact matches were excluded. The results of these self-alignments within this region were then summarized for every 1 kb window and visualized using the Gepard software.[19]

Results

A new rare recurrent deletion encompassing the most distal part of the long arm of Chromosome 1, del(1)(q42.2qter), was detected in 6 primary tumors (6/188, 3.2%) and one cell line (SK-N-FI, 1/33, 3.0%) (Fig. 1, Supporting Information Fig. S1). For six out of seven deletions, the breakpoints were identical at 10-kb resolution. The deletion was confirmed in SK-N-FI by FISH analysis and on a high resolution 1M array (Fig. 1, Supporting Information Fig. S2), whereas M-FISH excluded the presence of a balanced chromosomal rearrangement affecting 1q, at least at this resolution (data not shown). To further delineate the genomic characteristics of these 1q deletions and the clinical features linked to these tumors, we collected three additional cases from an unpublished independent tumor series analyzed with the same platform (3/113, 2.7%). Furthermore, we screened previously published datasets[20–22] to look for the presence of this particular rearrangement, yielding 10 additional cases with a similar 1q42.2-1qter deletion (for details see Supporting Information Table 4). Overall, the frequency of 1q deletions across these five tumor sample sets was 2.8% (19/679).

Investigation of the clinical and genomic features of the tumors carrying this particular deletion showed a significant association with high stage ($p = 0.003$) and the majority of 1q deleted tumors also exhibited 11q deletions (13/19 tumors with 1q deletion versus 154/657 tumors without 1q deletion; $p = 5.61 \times 10^{-5}$). This pointed out that 8% of 11q deleted tumors presented with a cooccurrence of the distal 1q deletion. Other genomic features significantly enriched amongst the distal 1q deleted samples are proximal 1q gain in 9/19 cases ($p = 5.29 \times 10^{-5}$; Supporting Information Fig. S3) and 19q deletion in 9/19 ($p = 5.51 \times 10^{-6}$) cases (for detailed statistics, see Table 1, Supporting Information Table 5). Within the 11q deleted high risk group, there was no significant difference in survival between samples with or without the 1q deletion (Supporting Information Fig. S4).

Breakpoint analysis at intermediary resolution level revealed a similar genomic localization in 5 out of the 13 additional cases compared to the cases profiled on our 44K/60K oligonucleotide array platform. In three remaining cases, breakpoints were positioned in a region ranging from 0.8 to 2.1 Mb proximal to the recurrent breakpoint, whereas for the other five samples no base pair positions of the breakpoints were available. Next, an ultrahigh density oligonucleotide array platform, covering the breakpoint on 1q was designed to perform a more detailed breakpoint analysis on 11 cases (see Supporting Information Table 4). This approach enabled us to fine map the breakpoint in each of these samples near to base pair level. Nine breakpoints clustered to a "hotspot" region within a 12.5-kb segment (genomic positions 229321385–229333895) whereas the

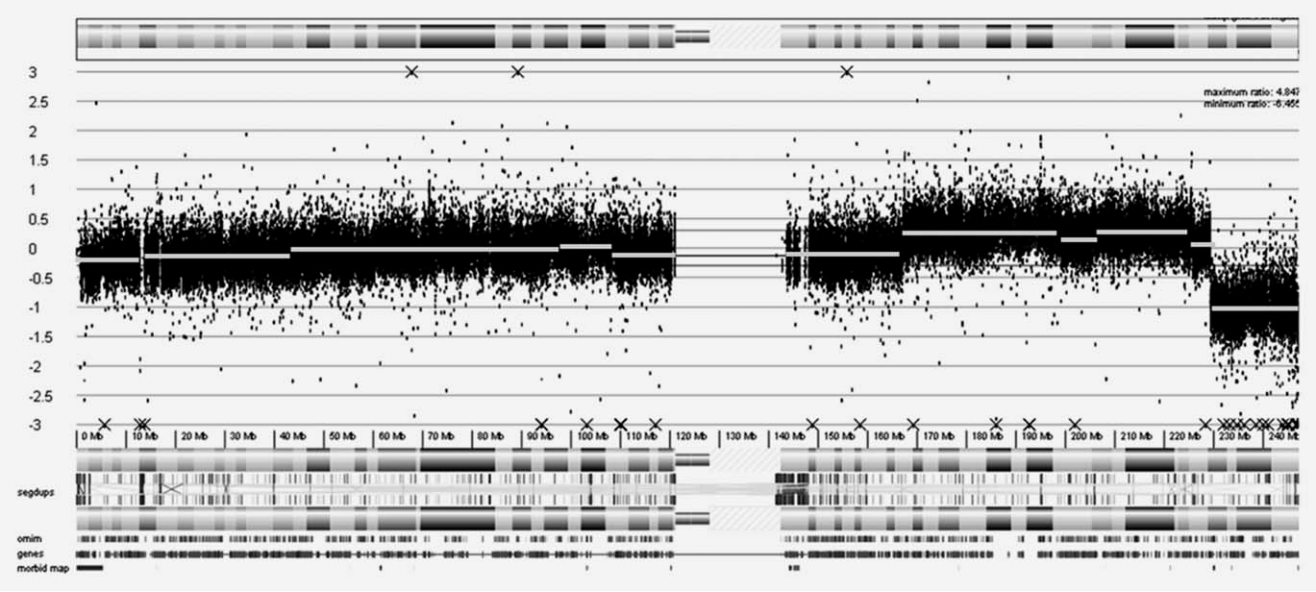

Figure 1. Array CGH profile of Chromosome 1 of the NB cell line SK-N-FI using the ultra-high resolution 1M oligonucleotide array platform. The deletion is evident at the distal end of the q-arm, preceded by a proximal 1q gain. The white lines on the tumor profile represent the CBS segments.

Table 1. Distribution of clinical parameters (stage, age) and primary genomic alterations (MYCN amplification, 11q and 19q deletion and 1q gain) for the total patient cohort analyzed in this study

	All samples	Samples with distal 1q deletion	Samples without distal 1q deletion	*p*-value (Fisher exact test)
Number (%)	677	19 (3)	658 (97)	
Tumor stage	651	19	632	
1, 2, 4S	233 (36)	1 (5)	232 (37)	0.003
3, 4	418 (64)	18 (95)	400 (63)	
Age	499	13	486	
>12 months	340 (68)	12 (92)	328 (67)	0.071
<12 months	159 (32)	1 (8)	158 (33)	
***MYCN* status**	677	19	658	
MYCN amplification	155 (23)	1 (5)	154 (23)	0.092
MYCN single copy	522 (77)	18 (95)	504 (77)	
11q status	676	19	657	
11q deletion	167 (25)	13 (68)	154 (23)	5.61×10^{-5}
No 11q deletion	509 (75)	6 (32)	503 (77)	
1q status	676	19	657	
Proximal 1q gain	74 (11)	9 (47)	65 (10)	5.29×10^{-5}
No proximal 1q gain	602 (89)	10 (53)	592 (90)	
19q status	676	19	657	
19q deletion	57 (8)	9 (47)	48 (7)	5.51×10^{-6}
no 19q deletion	619 (92)	10 (53)	609 (93)	

p-values were calculated using the Fisher exact test.

remaining two breakpoints were colocated 1.4-Mb proximal to this hotspot (genomic positions 227904200–227987941) (Fig. 2, Supporting Information Table 4). At this level of resolution, two pairs of identical breakpoints were found, situated between genomic position 229322024–229322239 and 229323891–229324551.

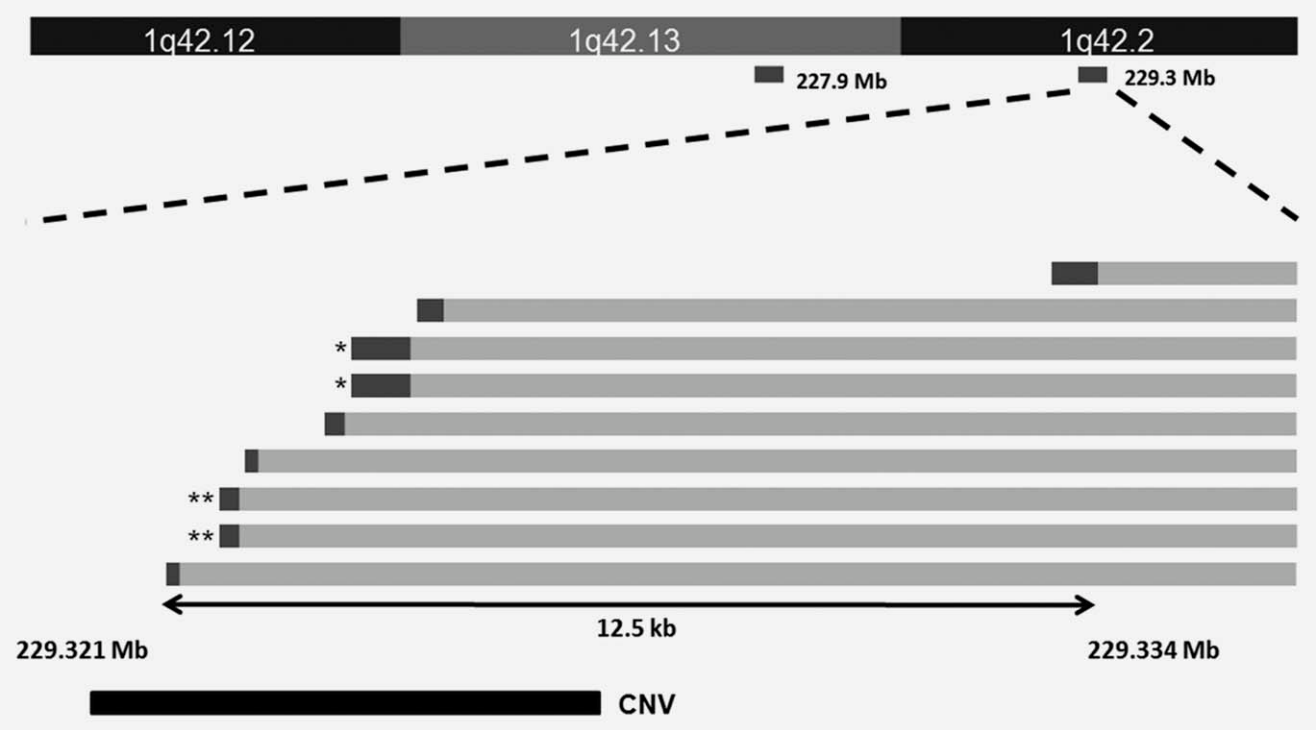

Figure 2. Schematic representation of the genomic position of the 11 chromosome 1q breakpoints as determined at a 115 bp resolution on the ultra-high resolution 1q array. The majority of breakpoints were found in the 'hotspot' position at position 229.3 Mb (in chromosome band 1q42.2). The two remaining breakpoints were located at genomic position 227.9 Mb in chromosome band 1q42.13. In the lower panel of the figure, the detailed positioning of the hotspot breakpoints at genomic position 229.3 Mb is depicted. The light grey bars represent the most proximal part of the deleted region and the dark grey bars represent the region between the last normal probe and the first deleted probe. The two pairs of breakpoints marked by * and **, respectively were located at identical breakpoint positions. The 7-kb copy number variable region is shown below on the figure.

The observed breakpoint hotspot prompted us to search for evidence for a possible underlying genomic structure driving the formation of these recurrent deletions. To this end, *in silico* analysis of the genomic region covering and flanking these breakpoints was performed. No segmental duplications were found in this region based on the most recent human genome assemblies (hg18 and hg19). Interestingly, 8 out of 11 breakpoints map to a 7-kb copy number variable region (chr1:229320471–229327610, hg18) recently detected by Sudmant *et al.*[23] in 159 human genomes sequenced using the Illumina platform. Using read-depth, the copy number of this region was detected as variable and contains between 3 and 5 copies in the genomes of different individuals. The human reference genome (hg18) contains this region duplicated five times based on read-depth analyses,[24] although no segmental duplications were detected by WGAC (whole genome assembly comparison) and Celera WSSD (whole genome shotgun sequence detection) analyses (Supporting Information Fig. S5). No copy number variable region could be detected in the region of the more proximal breakpoint cluster by this analysis, but we noted the presence of several LINE repeats and sequence similarities in the regions of the two breakpoint clusters detected (Supporting Information Fig. S6), thus possibly also rendering this particular region more prone to rearrangement.

The commonly deleted segment, defined by the most distal breakpoint, is 17.9 Mb in length and contains a total of 130 protein coding genes including a cluster of 27 olfactory receptor genes as well as one miRNA (hsa-miR-1537) and four T-UCRs (uc.43–uc.46). In the deletion interval, there were a total of 18 prioritized dosage sensitive genes identified, based on Spearman's correlation coefficient analysis for DNA copy number alterations and gene expression levels (p-value < 0.05). These dosage sensitive genes were further prioritized by selecting for genes with a fitSNP value larger than 0.55, which is indicative for genes that are more likely to harbor disease-associated variants.[25] Furthermore, inclusion in the NB gene server (NBGS database; Pattyn *et al.*, unpublished data) was also taken into account (Supporting Information Table 6). Fumarate hydratase (*FH*), a gene involved in familial hereditary leiomyomatosis and renal cell cancer[26] and with a known role in hypoxia, is one of these 18 genes. Mutation analysis of this gene in 32 NB cell lines and 9 primary NB tumors revealed one exonic mutation (p.Y491H), two intronic mutations of which one is initiating a start codon and three variants in the 3′UTR, possibly changing the

original binding site for miRNAs (Supporting Information Table 7). Another interesting gene located in this region, albeit not dosage sensitive, is *EGLN1* (EGL nine homolog 1) or *PHD2* (prolyl hydroxylase domain 2) which was recently described as a tumor suppressor gene in familial paraganglioma and breast cancer.[27,28] Mutation analysis in the same tumor panel revealed only one intronic variant in a NB cell line (Supporting Information Table 7).

MiRNA expression profiling was performed for hsa-mir-1537, the microRNA residing in the deletion and hsa-mir-1182, a microRNA just proximal to the breakpoint, on a cohort of 35 primary tumor samples, but these miRNAs were either very low or not expressed in the tested samples.

Discussion

Using high resolution array CGH screening on a large cohort of NB samples, we identified a rare recurrent 17.9-Mb terminal deletion on distal chromosome 1q (del(1)(q42.21qter)). Despite previous intensive DNA copy number analyses, this rearrangement was not previously reported. This may be explained by the relative low overall frequency of the alteration or by the lower sensitivity of BAC or other low resolution platforms that were previously used. Interestingly, retrospective analysis of selected previously (un)published datasets allowed identification of a total of 13 tumors with similar 1q breakpoints.

Upon analysis of the 1q deleted tumors from our series and the additionally identified cases, it became apparent that the majority occurred within the high risk NB Subtype 2A, which consists of 11q deleted tumors without *MYCN* amplification. This is in keeping with the fact that this major genomic subgroup of NB exhibits a higher number of structural aberrations as compared to *MYCN* amplified NB Subtype 2B.[21,22] It was suggested by the authors that these tumors exhibit a chromosomal instability phenotype possibly due to the loss of *H2AFX*, located on 11q.[21] However, we could not confirm their results regarding the lower expression of *H2AFX* in Subtype 2A tumors compared to the other subtypes, *H2AFX* mRNA expression levels were higher in Subtype 2B compared to both Subtypes 1 and 2A tumors, the latter two showing a similar expression level. Remarkably, the samples with the 1q deletion had a high expression level, comparable to the Subtype 2B tumors (Supporting Information Fig. S7).

In contrast to previously reported DNA copy number gains or losses in NB, the present distal 1q deletion breakpoints are not scattered but cluster within two defined genomic regions. In particular, 9 out of 11 breakpoints are located within a 12.5-kb segment as determined by ultra-high resolution DNA arrays (~115 bp resolution). *In silico* analysis of the breakpoint region revealed no segmental duplications; however, 8 out of 11 breakpoints were mapped to a 7-kb copy number variable region, suggesting a possible role for the underlying genomic architecture in the increased risk for double strand break formation.

Two possible candidate tumor suppressor genes located within the deleted segment are *FH* (fumarate hydratase) and *EGLN1* (EGL nine homolog 1). Both are *bona fide* tumor suppressor genes implicated in familial hereditary leiomyomatosis and renal cell cancer (*FH*)[26] and familial paraganglioma and breast cancer (*EGLN1*).[27,28] However, mutation analysis did not reveal further direct evidence for involvement of either of these two genes in our cohort of NB samples. Therefore further studies are needed to show whether haplo-insufficiency for both or either of the genes might contribute to the tumor phenotype.

The present finding is important for several reasons. First, we illustrate that upon analysis of a large tumor cohort with sufficiently high resolution for DNA copy number detection, new recurrent alterations can be detected. Such rare recurrent deletions may point at the presence of important tumor suppressor genes as recently illustrated for *PHF6* in T-ALL.[29] Currently, exome sequencing is ongoing to search for loss of function mutations for genes located within the 1q deleted segment. Second, the occurrence of rare genomic alterations detected by array CGH may be reminiscent to the low frequency mutations detected in whole genome sequencing projects. Subsequent data mining has indeed revealed that many of these apparently orphan mutations can be linked to common pathways specifically perturbed in particular tumor entities.[30] It can be anticipated that these rare 1q deletions may contribute to one or more commonly affected signaling pathways in NB. This was illustrated in our recent study uncovering DNA copy number alterations affecting multiple up and downstream components of the *MYCN* pathway (Kumps *et al.*, unpublished data). Thirdly, it occurred to us that in addition to *FH* and *EGLN1*, all other tumor suppressor genes predisposing to pheochromocytoma/paraganglioma map into regions that are commonly deleted in NB, and more specifically in NB tumors with a distal 1q deletion, such as *VHL* (von Hippel-Lindau) on 3p25.3, *SDHD* (succinate dehydrogenase complex, subunit D) on 11q23 and *SDHB* (succinate dehydrogenase complex, subunit B) on 1p36.13. Remarkably, these genes encode for consecutive enzymes in the Krebs cycle (*FH*, *SDHB* and *SDHD*), and are involved in the *HIF1A* hypoxia pathway (*FH*, *SDHB*, *SDHD*, *VHL*, *EGLN1*). A deficiency of these genes could lead to a stabilization of *HIF1A*, possibly leading to a so-called pseudohypoxic drive.[31]

In conclusion, as mentioned above, access to the detailed molecular portrait of tumors may turn out to be of critical importance for understanding responses of individual patients to new therapeutic strategies and pave the way for personalized targeted therapy.

Acknowledgement

C.K. is a predoctoral fellow indebted from the Agency for the Promotion of Innovation by Science and Technology (IWT-Vlaanderen); S.V. is a predoctoral fellow supported by a fellowship of the Research Foundation—Flanders (FWO); F.P. and K.D.P. are postdoctoral fellows of the Research Foundation—Flanders (FWO); R.L.S. is supported by Science Foundation Ireland

(07/IN.1/B1776) and the Children's Medical and Research Foundation, and P.H.S. is supported by a Natural Sciences and Engineering Research Council of Canada Fellowship. Furthermore, we acknowledge the support of the Belgian Foundation Against Cancer (Foundation of public interest), the Belgian program of Interuniversity Poles of Attraction (initiated by the Belgian State, Prime Minister's Office, Science Policy Programming), the Neuroblastoma Research Consortium and the National Genome Research Initiative (NGFN, German Ministry for Research and Education).

References

1. Brodeur GM. Neuroblastoma: biological insights into a clinical enigma. *Nat Rev Cancer* 2003;3:203–16.
2. Van Roy N, De Preter K, Hoebeeck J, Van Maerken T, Pattyn F, Mestdagh P, Vermeulen J, Vandesompele J, Speleman F. The emerging molecular pathogenesis of neuroblastoma: implications for improved risk assessment and targeted therapy. *Genome Med* 2009;1:74.
3. Piccaluga PP, Rondoni M, Paolini S, Rosti G, Martinelli G, Baccarani M. Imatinib mesylate in the treatment of hematologic malignancies. *Expert Opin Biol Ther* 2007; 7:1597–611.
4. Tsao MS, Sakurada A, Cutz JC, Zhu CQ, Kamel-Reid S, Squire J, Lorimer I, Zhang T, Liu N, Daneshmand M, Marrano P, da Cunha Santos G, et al. Erlotinib in lung cancer—molecular and clinical predictors of outcome. *N Engl J Med* 2005;353: 133–44.
5. Van Maerken T, Speleman F, Vermeulen J, Lambertz I, De Clercq S, De Smet E, Yigit N, Coppens V, Philippe J, De Paepe A, Marine JC, Vandesompele J. Small-molecule MDM2 antagonists as a new therapy concept for neuroblastoma. *Cancer Res* 2006;66:9646–55.
6. Heidorn SJ, Milagre C, Whittaker S, Nourry A, Niculescu-Duvas I, Dhomen N, Hussain J, Reis-Filho JS, Springer CJ, Pritchard C, Marais R. Kinase-dead BRAF and oncogenic RAS cooperate to drive tumor progression through CRAF. *Cell* 2010;140:209–21.
7. Cohn SL, Pearson ADJ, London WB, Monclair T, Ambros PF, Brodeur GM, Faldum A, Hero B, Iehara T, Machin D, Mosseri V, Simon T, et al. The international neuroblastoma risk group (INRG) classification system: an INRG task force report. *J Clin Oncol* 2009;27:289–97.
8. Michels E, Vandesompele J, De Preter K, Hoebeeck J, Vermeulen J, Schramm A, Molenaar JJ, Menten B, Marques B, Stallings RL, Combaret V, Devalck C, et al. ArrayCGH-based classification of neuroblastoma into genomic subgroups. *Gene Chromosome Cancer* 2007;46: 1098–108.
9. Vandesompele J, Baudis M, De Preter K, Van Roy N, Ambros P, Bown N, Brinkschmidt C, Christiansen H, Combaret V, Lastowska M, Nicholson J, O'Meara A, et al. Unequivocal delineation of clinicogenetic subgroups and development of a new model for improved outcome prediction in neuroblastoma. *J Clin Oncol* 2005;23:2280–99.
10. Janoueix-Lerosey I, Schleiermacher G, Michels E, Mosseri V, Ribeiro A, Lequin D, Vermeulen J, Couturier J, Peuchmaur M, Valent A, Plantaz D, Rubie H, et al. Overall genomic pattern is a predictor of outcome in neuroblastoma. *J Clin Oncol* 2009;27:1026–33.
11. Olshen AB, Venkatraman ES, Lucito R, Wigler M. Circular binary segmentation for the analysis of array-based DNA copy number data. *Biostatistics* 2004;5:557–72.
12. van de Wiel MA, Brosens R, Eilers PH, Kumps C, Meijer GA, Menten B, Sistermans E, Speleman F, Timmerman ME, Ylstra B. Smoothing waves in array CGH tumor profiles. *Bioinformatics* 2009; 25:1099–104.
13. Menten B, Pattyn F, De Preter K, Robbrecht P, Michels E, Buysse K, Mortier G, De Paepe A, van Vooren S, Vermeesch J, Moreau Y, De Moor B, et al. arrayCGHbase: an analysis platform for comparative genomic hybridization microarrays. *BMC Bioinform* 2005;6:124.
14. Van Roy N, Laureys G, Van Gele M, Opdenakker G, Miura R, van der Drift P, Chan A, Versteeg R, Speleman F. Analysis of 1;17 translocation breakpoints in neuroblastoma: implications for mapping of neuroblastoma genes. *Eur J Cancer* 1997;33:1974–8.
15. Van Limbergen H, Poppe B, Michaux L, Herens C, Brown J, Noens L, Berneman Z, De Bock R, De Paepe A, Speleman F. Identification of cytogenetic subclasses and recurring chromosomal aberrations in AML and MDS with complex karyotypes using M-FISH. *Genes Chromosomes Cancer* 2002;33:60–72.
16. Mestdagh P, Bostrom AK, Impens F, Fredlund E, Van Peer G, De Antonellis P, von Stedingk K, Ghesquiere B, Schulte S, Dews M, Thomas-Tikhonenko A, Schulte JH, et al. The miR-17-92 microRNA cluster regulates multiple components of the TGF-beta pathway in neuroblastoma. *Mol Cell* 2010;40:762–73.
17. Mestdagh P, Feys T, Bernard N, Guenther S, Chen C, Speleman F, Vandesompele J. High-throughput stem-loop RT-qPCR miRNA expression profiling using minute amounts of input RNA. *Nucleic Acids Res* 2008;36:e143.
18. Mestdagh P, Van Vlierberghe P, De Weer A, Muth D, Westermann F, Speleman F, Vandesompele J. A novel and universal method for microRNA RT-qPCR data normalization. *Genome Biol* 2009;10:R64.
19. Krumsiek J, Arnold R, Rattei T. Gepard: a rapid and sensitive tool for creating dotplots on genome scale. *Bioinformatics* 2007;23:1026–8.
20. Buckley PG, Alcock L, Bryan K, Bray I, Schulte JH, Schramm A, Eggert A, Mestdagh P, De Preter K, Vandesompele J, Speleman F, Stallings RL. Chromosomal and microRNA expression patterns reveal biologically distinct subgroups of 11q-neuroblastoma. *Clin Cancer Res* 2010;16: 2971–8.
21. Caren H, Kryh H, Nethander M, Sjoberg RM, Trager C, Nilsson S, Abrahamsson J, Kogner P, Martinsson T. High-risk neuroblastoma tumors with 11q-deletion display a poor prognostic, chromosome instability phenotype with later onset. *Proc Natl Acad Sci USA* 2010;107:4323–8.
22. Mosse YP, Diskin SJ, Wasserman N, Rinaldi K, Attiyeh EF, Cole K, Jagannathan J, Bhambhani K, Winter C, Maris JM. Neuroblastomas have distinct genomic DNA profiles that predict clinical phenotype and regional gene expression. *Genes Chromosomes Cancer* 2007;46: 936–49.
23. Sudmant PH, Kitzman JO, Antonacci F, Alkan C, Malig M, Tsalenko A, Sampas N, Bruhn L, Shendure J, Eichler EE. Diversity of human copy number variation and multicopy genes. *Science* 2010;330:641–6.
24. Alkan C, Kidd JM, Marques-Bonet T, Aksay G, Antonacci F, Hormozdiari F, Kitzman JO, Baker C, Malig M, Mutlu O, Sahinalp SC, Gibbs RA, et al. Personalized copy number and segmental duplication maps using next-generation sequencing. *Nat Genet* 2009;41:1061–7.
25. Chen R, Morgan AA, Dudley J, Deshpande T, Li L, Kodama K, Chiang AP, Butte AJ. FitSNPs: highly differentially expressed genes are more likely to have variants associated with disease. *Genome Biol* 2008; 9:R170.
26. Refae MA, Wong N, Patenaude F, Begin LR, Foulkes WD. Hereditary leiomyomatosis and renal cell cancer: an unusual and aggressive form of hereditary renal carcinoma. *Nat Clin Pract Oncol* 2007;4:256–61.
27. Bordoli MR, Stiehl DP, Borsig L, Kristiansen G, Hausladen S, Schraml P, Wenger RH, Camenisch G. Prolyl-4-hydroxylase PHD2- and hypoxia-inducible factor 2-dependent regulation of

amphiregulin contributes to breast tumorigenesis. *Oncogene* 2011;30:548–60.
28. Ladroue C, Carcenac R, Leporrier M, Gad S, Le Hello C, Galateau-Salle F, Feunteun J, Pouyssegur J, Richard S, Gardie B. PHD2 mutation and congenital erythrocytosis with paraganglioma. *N Engl J Med* 2008; 359:2685–92.
29. Van Vlierberghe P, Palomero T, Khiabanian H, Van der Meulen J, Castillo M, Van Roy N, De Moerloose B, Philippe J, Gonzalez-Garcia S, Toribio ML, Taghon T, Zuurbier L, et al. PHF6 mutations in T-cell acute lymphoblastic leukemia. *Nat Genet* 2010;42:338–42.
30. Sjoblom T, Jones S, Wood LD, Parsons DW, Lin J, Barber TD, Mandelker D, Leary RJ, Ptak J, Silliman N, Szabo S, Buckhaults P, et al. The consensus coding sequences of human breast and colorectal cancers. *Science* 2006;314: 268–74.
31. Pollard PJ, Briere JJ, Alam NA, Barwell J, Barclay E, Wortham NC, Hunt T, Mitchell M, Olpin S, Moat SJ, Hargreaves IP, Heales SJ, et al. Accumulation of Krebs cycle intermediates and over-expression of HIF1alpha in tumours which result from germline FH and SDH mutations. *Hum Mol Genet* 2005;14:2231–9.